# Ground state structure of high-energy-density polymeric carbon monoxide

Kang Xia,[1] Jian Sun,[1,*] Chris J. Pickard,[2,3] Dennis D. Klug,[4] and Richard J. Needs[5]

[1] *National Laboratory of Solid State Microstructures, School of Physics and Collaborative Innovation Center of Advanced Microstructures, Nanjing University, Nanjing, 210093, P. R. China*

[2] *Department of Materials Science & Metallurgy, University of Cambridge, 27 Charles Babbage Road, Cambridge CB3 0FS, UK*

[3] *Advanced Institute for Materials Research, Tohoku University 2-1-1 Katahira, Aoba, Sendai, 980-8577, Japan*

[4] *Steacie Institute for Molecular Sciences, National Research Council of Canada, Ottawa, K1A 0R6, Canada*

[5] *Theory of Condensed Matter Group, Cavendish Laboratory, J J Thomson Avenue, Cambridge CB3 0HE, UK*

(Dated: March 10, 2017)

Crystal structure prediction methods and first-principles calculations have been used to explore low-energy structures of carbon monoxide (CO). Contrary to the standard wisdom, the most stable structure of CO at ambient pressure was found to be a polymeric structure of $Pna2_1$ symmetry rather than a molecular solid. This phase is formed from six-membered (4 Carbon + 2 Oxygen) rings connected by C=C double bonds with two double-bonded oxygen atoms attached to each ring. Interestingly, the polymeric $Pna2_1$ phase of CO has a much higher energy density than trinitrotoluene (TNT). On compression to about 7 GPa, $Pna2_1$ is found to transform into another chain-like phase of $Cc$ symmetry which has similar ring units to $Pna2_1$. On compression to 12 GPa, it is energetically favorable for CO to polymerize into a purely single-bonded $Cmca$ phase, which is stable over a wide pressure range and transforms into the previously known $Cmcm$ phase at around 100 GPa. Thermodynamic stability of these structures was verified using calculations with different density functionals, including hybrid and van der Waals corrected functionals.

## I. INTRODUCTION

Carbon monoxide (CO) has the strongest known chemical bond. It has been used extensively as a probe molecule for investigating oxidation reactions in catalysis, and it is an important industrial gas. The study of polymerization of molecular crystals[1,2] is essential for understanding their fundamental physics and chemistry, and for discovering new materials with useful properties such as "high energy density"[3] and "superhardness"[4,5]. The phase diagram and polymerization of CO have consequently been studied in depth over several decades[3,6–16]. Transformations from van der Waals bonded molecular phases to covalently bonded networks have been explored in similar systems, such as $N_2$[17,18], $O_2$[19], CO[12,13], and $CO_2$[20,21].

The triple bond in CO can be broken quite readily under pressure, and it can polymerize at rather low pressures and temperatures. For example, Raman spectroscopy studies have found that molecular CO polymerizes at a pressure of 4–5 GPa and temperatures >80 K[6,8]. The product reacts photochemically with visible laser light and the transformation is reversible at ambient conditions. Polymerization of CO via the breaking of triple bonds leading to the formation of C=C bonds has also been studied[12,14]. Lipp *et al.* recently reported that the Fourier transform infra-red (FTIR) spectrum of solid polymeric CO (p-CO), which decomposes explosively into $CO_2$ and glassy carbon, might be explained by rings containing –C–O–(C=O)–C– units. Ceppatelli *et al.*[15] found that an extended amorphous material forms from polycarbonyl chains at temperatures <300 K, while above room temperature polycarbonyl chains decompose into carbon dioxide and epoxy rings.

On the other hand, in previous work, a metallic zigzag polymeric chain-like CO material was found to be more stable than molecular CO at ambient pressure[16]. This structure of $P2_1/m$ symmetry is formed from polycarbonyl chains containing a mixture of single and double bonds. Although not crystalline, chain-like structures consisting of five CO molecules have been successfully synthesized using organic chemistry methods[22]. However, according to Peierls' distortion theorem[23], one-dimensional metallic chains are unstable to a distortion which opens up a band gap between the occupied and unoccupied electronic states. Although weak interactions between chains in solid $P2_1/m$ persist, one might suspect that a Peierls' distortion to an insulating structure could be energetically favorable in polymeric CO.

It is widely accepted that molecular gases such as CO, $N_2$ and $CO_2$ are likely to be more stable at ambient pressure than their polyermized counterparts. However, a very few exceptions have recently been discovered. For example, Wen *et al.*[24] found graphane sheets to be energetically more stable than benzene under pressure. Within the same 1:1 stoichiometry as CO, the crystal structure of silicon monoxide was explored theoretically and similar crystalline structures to those of CO were predicted[25]. However, recent experiments on amorphous SiO found evidence of atomic-scale disproportionation and suboxide-type tetrahedral coordination[26]. It is also worth mentioning that CO is likely to be the second most abundant molecule in interstellar space[27,28]. The existence of molecular CO gas was newly discovered

in extremely metal-poor galaxies[29]. It is suggested to be present in dust or grains found in dense molecular clouds, and low pressure polymeric structures of CO may therefore exist.

## II. METHODS

Searches for CO at high pressures were performed using the ab inition random structure searching (AIRSS) method. A plane wave cutoff energy of 700 eV was used, with a k-point grid of spacing less than $2\pi\times0.05$ Å$^{-1}$. AIRSS has predicted new structures that have subsequently been verified experimentally, including compounds of carbon and oxygen[30–34], and recently several quantum materials[35–37]. For example, a new stable structure of $FeO_2$[38] predicted using AIRSS was identified very recently in experiments performed at pressures found in the Earth's lower mantle[39].

Large cell searches with up to 32 atoms were carried out to include the possibility of more complicated structures. The stability of CO structures was investigated using first-principles DFT methods, the projector-augmented wave method (PAW)[40,41] as implemented in the VASP code[42], a plane wave basis set, and a generalized gradient approximation (GGA) functional. In most computations the electronic wave functions were expanded in a plane wave basis set with a kinetic energy cutoff of 1050 eV and integrals over the Brillouin zone were sampled using a k-point grid of spacing $<0.03\times2\pi$ Å$^{-1}$. The hard version PAW Perdew-Burke-Ernzerhof (PBE) potentials[43] for C and O were used. The vibrational modes and frequencies of the most stable structures were calculated. A density-functional perturbation theory (DFPT) approach[44] and the QUANTUM-ESPRESSO code[45] were employed to calculate the phonon modes and frequencies with a kinetic energy cutoff of 1088 eV and an $(8\times8\times8)$ k-point grid, together with the semiempirical dispersion correction of Grimme's DFT-D2[46] scheme. An *ab-initio* molecular dynamics (AIMD) simulation of 1.2 pico-second duration at 0 GPa and 300 K was used to further test the stability of the $Pna2_1$ structure. These calculations were performed using Parrinello-Rahman ($NpT$) dynamics[47,48] with a Langevin thermostat, a time-step of 1 fs and a kinetic energy cutoff of 910 eV in a $(1\times3\times2)$ supercell with 96 CO formula units (f.u.).

## III. RESULTS

Using the *ab initio* random structure searching (AIRSS) method[49,50], we predict that several new CO structures are energetically more stable than previously-known ones over a wide range of pressures. Among them we find a chain-like polymeric phase consisting of six-membered rings (space group: $Pna2_1$) at ambient pressures to be more stable than the molecular phases. More importantly, we find that polymeric $Pna2_1$-CO is a potential "high energy density" material, which can release about 4–9 times more energy than Trinitrotoluene (TNT), if it decomposes into carbon+$CO_2$ or reacts with oxygen and converts into $CO_2$.

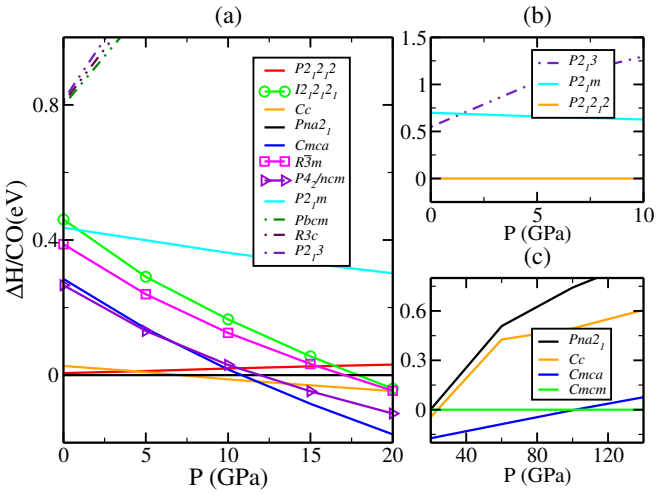


FIG. 1: Enthalpy-pressure relations for CO structures. (a) Enthalpies of the most relevant structures at low pressures <20 GPa relative to $Pna2_1$. (b) Three representative structures (one molecular phase, two chain-like structures) at low pressures <10 GPa relative to the $P2_12_12$ phase calculated using the hybrid HSE06 functional[51–54] plus the zero-point energy. The $P2_12_12$ structure is chosen as the reference due to the prohibitive cost of calculations for $Pna2_1$. (c) At high pressures up to 140 GPa relative to $Cmcm$. The kinks result from sudden volume changes during compression. Calculations for (a) and (c) were performed with the PBE functional together with the DFT-D3 correction using the Becke-Jonson (BJ) damping function parameters of Grimme *et al.*[55,56] Dashed lines represent the molecular phases, solid lines with symbols represent the framework and layered structures, and solid lines represent the chain-like structures.

Structure searches were performed using the CASTEP[57] code and the AIRSS approach[49,50], and structural optimizations with higher accurcy criteria were performed with VASP[42] for cross checking. Previous work has shown that dispersion corrections for molecular and layered systems must be included to obtain accurate lattice constants[35,37]. We have investigated several commonly used dispersion corrections implemented in the VASP[42], as listed in TABLE I. The errors in the lattice constants with the standard PBE functional are large, but they are much reduced when a van der Waals corrected functional is used. Grimme's DFT-D3 (BJ-damping) method[55,56] combined with the PBE functional (PBE-D3) gives the smallest error for molecular systems such as CO and $CO_2$, while the optB88 functional[58–61] together with the vdW-DF corrections of Langreth and Lundqvist *et al.*[62] gives the most accurate results for the inter-layer separations of graphite and crystalline $MoS_2$.

| exchange-correlation | PBE/err.(%) | vdW-DF2/err.(%) | optB88-vdW/err.(%) | PBE-D3/err.(%) | Exp. |
|---|---|---|---|---|---|
| $\alpha$-CO | 6.093/8.2 | 5.502/2.3 | 5.447/3.3 | 5.634/0.07 | 5.630[63] |
| $\alpha$-$CO_2$ | 5.944/5.7 | 5.538/1.5 | 5.432/3.4 | 5.644/0.4 | 5.624[64] |
| graphite | 37.592/12.4 | 34.775/4.0 | 33.442/0.02 | 33.717/0.8 | 33.450[65] |
| $MoS_2$ | 13.399/9.0 | 12.956/5.4 | 12.500/1.7 | 12.077/1.8 | 12.294[66] |

TABLE I: Lattice constants in Å for a variety of solids calculated using VASP and different exchange-correlation functionals. The structures were optimised using PBE-D3(BJ-damping)[43,55,56], and two other vdW-DF corrections (optB88-vdW[58–61] and the rPW86 functional with the vdW-DF2 correction[62,67]) and the PBE functional[43]. Experimental lattice constants for the molecular $\alpha$-CO and $\alpha$-$CO_2$ phases were obtained from Vegard *et al.*[63] and Simon *et al.*[64] including interlayer distances of graphite from Nixon *et al.*[65] and layered $MoS_2$ (space group $P6_3/mmc$) from Bronsema *et al.*[66]. For comparison, we list the absolute values and relative errors (err.) for each structure. For the molecular systems, the error arising from the PBE-D3 correction is smaller than that from the PBE functional and vdW-DF2 correction.

CO is relatively unstable compared to graphite and $CO_2$ in an oxygen rich environment. However, here we restrict ourselves to an oxygen poor environment and focus only on the 1:1 stoichiometry. Enthalpy-pressure relations for the most relevant CO structures are shown in Fig. 1. Calculations using the PBE-D3 (BJ) functional suggest that at least four structures, including $P2_12_12$, $Pna2_1$, $Cc$, and $Cmca$ are more stable than the previously predicted zig-zag chain-like $P2_1/m$ structure[16]. Among them, as shown in Fig. 1(a), the polymeric chain-like $Pna2_1$ structure has an enthalpy of about 0.436 eV/CO lower than that of $P2_1/m$, and about 0.814 eV/CO lower than the molecular $\alpha$-CO structure (space group: $P2_13$) at 0 GPa. $Pna2_1$-CO is predicted to transform into the $Cc$ structure at pressures of about 7.1 GPa. With further compression, another chain-like structure of $Cmca$ symmetry is predicted to be stable in a wide pressure range of about 12–100 GPa, as can be seen in Fig. 1(c). Calculations with the HSE06 hybrid functional[51–54] plus the zero-point energy (ZPE) using the quasi-harmonic approximation support the conclusion that the polymeric chain-like $P2_12_12$-CO and $Pna2_1$-CO are much more stable than the molecular CO phase and the previous polymeric $P2_1/m$ structure at pressures below 10 GPa. To investigate the robustness of our results we calculated the enthalpies with commonly used functionals including PBE, PBE+vdW-DF2, and optB88-vdW. In each case we found the polymeric chain-like $Pna2_1$ structure to be the most stable phase at low pressures. Additional phase transitions occur at higher pressures.

Since $Pna2_1$-CO is thermodynamically much more favorable than molecular CO, it has a much higher energy density than molecular CO. We calculate that one kilogram of $Pna2_1$-CO can release about 16.2 megajoules of energy when it decomposes into graphite and $\alpha$-$CO_2$. (The energy of 1 kg TNT is about 4.2 megajoule.) If $Pna2_1$-CO reacts with oxygen and converts completely into $CO_2$, it can release up to about 37.3 megajoules of energy.

As shown in the crystal structure in Fig. 3(b), $Pna2_1$ is a chain-like structure consisting of six-membered rings connected by C=C double bonds. Each six-membered ring contains four carbon atoms and two oxygen atoms,

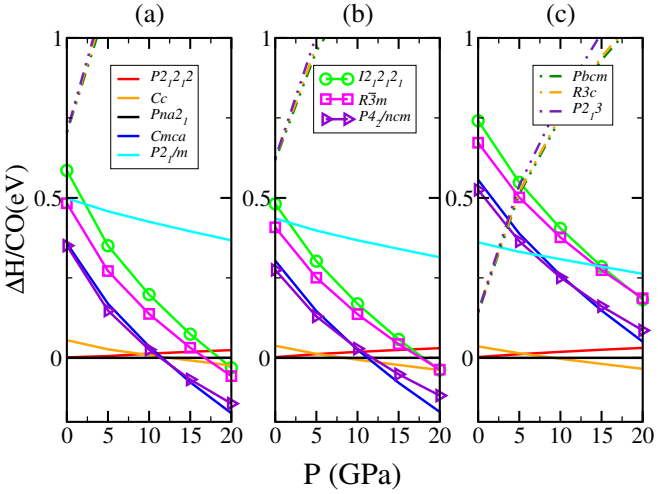


FIG. 2: Static lattice enthalpy-pressure relations for CO structures calculated using various exchange-correlation functionals. (a) PBE[43], (b) optB88-vdW[58–61], (c) vdW-DF2[62,67]. Dashed lines represent the molecular phases, solid lines with marks represent the framework and layered structures, and solid lines represent the chain-like structures. Note that the labels are separated into three parts in the three panels.

and two additional oxygen atoms are attached to two carbon atoms in the ring to form two C=O carbonyl groups, as shown in Fig. 3(e). Structures optimized at 0 GPa using the PBE-D3 (BJ) functional have single-bond lengths in the range 1.309–1.455 Å, while the C=C bond length is 1.413 Å and the shorter C=O bond is of length 1.200 Å. As shown in Fig. 3(a) and (c), in addition to the $Pna2_1$ phase we have found two other conformations of similar structures with six-membered rings ($P2_12_12$ and $Cc$). The higher pressure $Cmca$ structure is composed of units similar to the single-bonded $I2_12_12_1$ phase, as can be seen in Fig. 3(d). The optimized lattice parameters of the most relevant structures are listed in TABLE II.

The $Pna2_1$-CO structure (16 f.u.), $P2_12_12$ (8 f.u.), and $Cc$ (8 f.u.) have very similar structures featuring six-membered rings. Phonon calculations for the $Pna2_1$ structure are expensive, and we have therefore instead calculated the phonon dispersion curves of the closely re-

| Space Group (ITN) | Lattice Parameters a(Å) | b(Å) | c(Å) | Wyckoff Positions | | | | |
|---|---|---|---|---|---|---|---|---|
| $P2_12_12$(No. 18) | 8.079 | 5.434 | 4.197 | C(1) | 4c: | 0.4161 | 0.3064 | 0.9073 |
| | | | | C(2) | 2a: | 0.0000 | 0.0000 | 0.2615 |
| | | | | C(3) | 2a: | 0.5000 | 0.5000 | 0.4020 |
| | | | | O(1) | 4c: | 0.8314 | 0.3600 | 0.1861 |
| | | | | O(2) | 4c: | 0.0577 | 0.8078 | 0.7499 |
| $Pna2_1$(No. 33) | 10.472 | 4.198 | 8.241 | C(1) | 4a: | 0.7263 | 0.9122 | 0.3328 |
| | | | | C(2) | 4a: | 0.6257 | 0.7441 | 0.2505 |
| | | | | C(3) | 4a: | 0.6256 | 0.4075 | 0.2506 |
| | | | | C(4) | 4a: | 0.5257 | 0.9129 | 0.1673 |
| | | | | O(1) | 4a: | 0.4407 | 0.8202 | 0.0820 |
| | | | | O(2) | 4a: | 0.8129 | 0.8188 | 0.4153 |
| | | | | O(3) | 4a: | 0.7254 | 0.2557 | 0.3071 |
| | | | | O(4) | 4a: | 0.5258 | 0.2554 | 0.1944 |
| $Cc$(No. 9) | 6.785 | 5.079 $\beta$=132.681° | 13.797 | C(1) | 4a: | -0.4126 | 0.3997 | -0.3395 |
| | | | | C(2) | 4a: | -0.9452 | -0.0490 | -0.2486 |
| | | | | C(3) | 4a: | -0.6139 | 0.2840 | -0.2492 |
| | | | | C(4) | 4a: | -0.8171 | 0.1724 | -0.1605 |
| | | | | O(1) | 4a: | -0.3340 | -0.2416 | -0.0855 |
| | | | | O(2) | 4a: | -0.4957 | 0.2264 | -0.4174 |
| | | | | O(3) | 4a: | -0.7418 | 0.0913 | -0.3347 |
| | | | | O(4) | 4a: | -0.6396 | 0.3268 | -0.1646 |
| $Cmca$(No. 64) | 6.808 | 11.079 | 3.399 | C | 16g: | 0.3203 | -0.4332 | 1.0647 |
| | | | | O(1) | 8e: | 0.2500 | 0.8629 | 1.2500 |
| | | | | O(2) | 8f: | 0.0000 | -0.8905 | 1.2043 |
| $Pbcm$(No. 57) | 3.447 | 8.279 | 12.781 | C(1) | 8e: | 0.3669 | 0.5603 | -0.8480 |
| | | | | C(2) | 4d: | -0.4743 | 0.8089 | -0.7500 |
| | | | | C(3) | 4d: | 0.4369 | 0.6435 | 0.2500 |
| | | | | O(1) | 8e: | 0.2700 | 0.6089 | -0.5688 |
| | | | | O(2) | 8e: | 0.4190 | 0.3833 | -0.8396 |
| $Cmmm$(No. 65) | 10.993 | 4.960 | 5.030 | C(1) | 8o: | 0.5729 | 0.5000 | 0.8426 |
| | | | | C(2) | 8q: | 0.6909 | 0.6640 | 0.5000 |
| | | | | O | 16r: | 0.6273 | 0.2725 | 0.2670 |
| $I4_1/amd$(No. 141) | 7.036 | 7.036 | 4.809 | C | 32i: | 0.1753 | 0.3247 | 0.7500 |
| | | | | O | 32i: | 0.8040 | 0.5000 | 0.6149 |
| $P4_2mc$(No. 105) | 4.816 | 4.816 | 5.577 | C(1) | 4e: | 0.5000 | 0.8299 | 0.0873 |
| | | | | C(2) | 4e: | 0.6693 | 0.5000 | 0.3445 |
| | | | | O | 8f: | 0.2672 | 0.2563 | 0.2193 |
| $Imma$(No. 74) | 4.762 | 4.971 | 11.167 | C(1) | 8i: | -0.1724 | 0.7500 | 0.6878 |
| | | | | C(2) | 8h: | 0.0000 | -0.9147 | 0.05772 |
| | | | | O | 16j: | 0.2563 | 0.5238 | 0.6217 |
| $P4_2/ncm$(No. 138) | 6.642 | 6.642 | 5.650 | C(1) | 8i: | 0.8334 | 0.6666 | 0.7612 |
| | | | | C(2) | 8i: | -0.5864 | 0.08637 | -0.01821 |
| | | | | O | 16j: | 0.2444 | -0.5045 | 0.8925 |
| $R\bar{3}m$(No. 166) | 9.195 | 9.195 | 7.541 | C(1) | 18h: | 0.2415 | 0.4830 | 0.7069 |
| | | | | C(2) | 18h: | 0.0851 | 0.1703 | 0.7412 |
| | | | | O(1) | 18h: | 0.1587 | 0.3175 | 0.6387 |
| | | | | O(1) | 18h: | 0.1678 | 0.0839 | 0.6800 |

TABLE II: Structure details for the newly predicted CO structures optimized at 0 GPa. ITN shows the International Crystallographic Table Number.

lated $P2_12_12$ structure at 0 GPa. As shown in Fig. 5, $P2_12_12$ does not have any negative (imaginary) phonon frequencies, and the structure is predicted to be dynamically stable at ambient pressure. The phonon modes of the $P2_12_12$ phase can be divided into three groups. The high frequency bands at around 1394–1420 and 1756–1815 cm$^{-1}$ arise from C=C and C=O stretching within the chain, which agrees with the FTIR-spectra measurements of Lipp *et al.*[3]. The intermediate frequency bands from 608 to 1207 cm$^{-1}$ arise from the C-O and C-C single bonds in the plane of the six-membered rings, while the frequencies below 602 cm$^{-1}$ mainly arise from inter-chain vibrations. The dispersionless bands along the Z–T, Y–X and U–R directions result from the parallel arrangement of the chains, showing that the interactions between the chains are weak. The dispersion relations are quite sim-

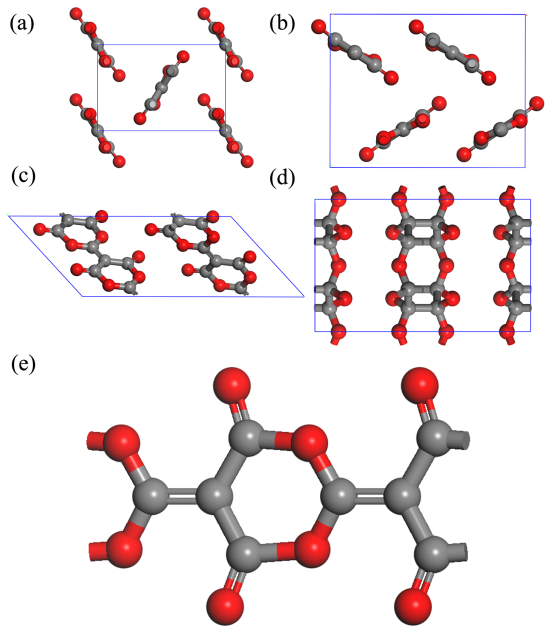


FIG. 3: The four best candidate structures for the ground state of polymeric CO at low pressures (grey color for C atoms and red for O atoms). (a) $P2_12_12$ viewed from [010], (b) $Pna2_1$ from [001], (c) $Cc$ from [010], (d) $Cmca$, (e) sketch of the single-chain with six-membered ring, which is the basic building block unit of $P2_12_12$, $Pna2_1$ and $Cc$.

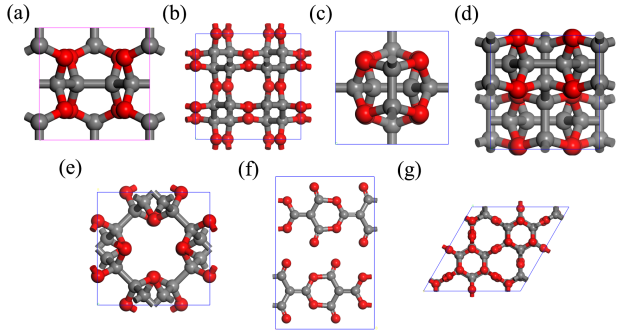


FIG. 4: Crystal structures of other CO phases (C=grey; O=red). (a) $Cmmm$, (b) $I4_1/amd$, (c) $P4_2mc$, (d) $Imma$, (e) $P4_2/ncm$, (f) $Pbcm$, (g) $R\bar{3}m$.

ilar to those found in the chain-like CO structures considered in earlier work[16].

The electronic band structure and density of states of $P2_12_12$ and $Pna2_1$ at 0 GPa, $Cc$ at 10 GPa and $Cmca$ at 15 GPa are shown in Fig. 6. Calculations with the PBE-D3 (BJ) functional[55,56] suggest that they are all semiconductors and that the polymeric chains $P2_12_12$ and $Pna2_1$ have band gaps of about 2.5–2.6 eV. However, the hybrid HSE06 functional is expected to give larger and more accurate gaps than semi-local functionals, and we take the band gap of 3.6 eV obtained with the HSE06 functional as our best estimate. We find that $P2_12_12$ and

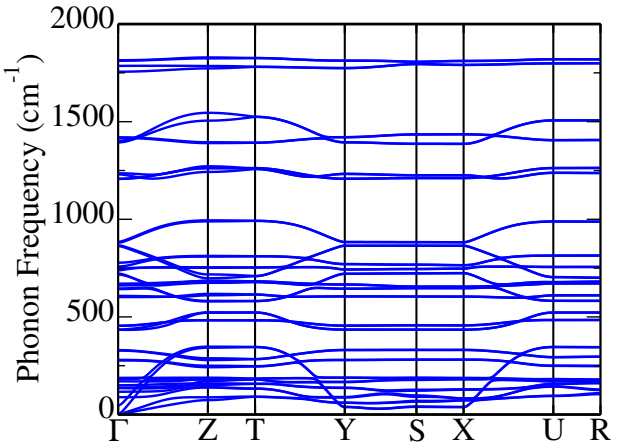


FIG. 5: Phonon dispersion relations of phase $P2_12_12$ of CO at 0 GPa.

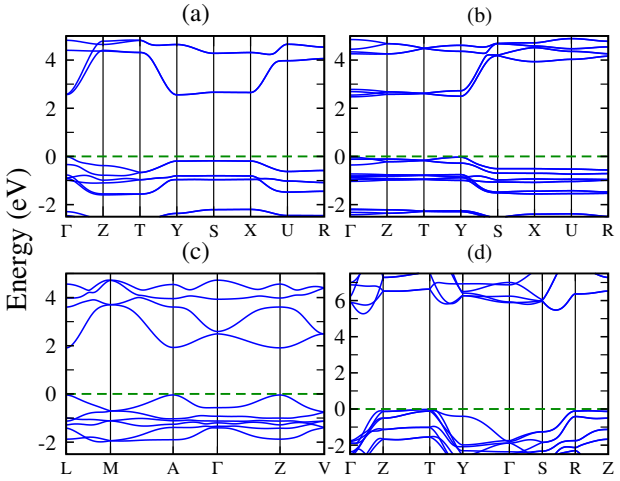


FIG. 6: Electronic band structures of four new polymeric phases, (a) $P2_12_12$ at 0 GPa, (b) $Pna2_1$ at 0 GPa, (c) $Cc$ at 10 GPa, and (d) $Cmca$ at 15 GPa. The top of the valence band is shown as a dashed line at zero energy. These calculations were performed using the optimised PBE-D3 (BJ) functionals[55,56].

$Pna2_1$ have direct band gaps at the Γ point, and they may be classified as large band-gap semiconductors and could be transparent. The bands of $P2_12_12$ along the Y–S–X direction at the top of the valence bands and bottom of the conduction bands are almost dispersionless, which indicates that the carriers have a large effective mass. The large carrier effective mass of $Pna2_1$ along a wide range of high symmetry directions (except Y–S) results from the weak inter-chain interactions that are similar to those in the $P2_12_12$ phase.

The enthalpy-pressure plots in Fig. 1 suggest that the chain-like $Pna2_1$-CO is energetically stable compared to molecular phases and the polycarbonyl chain-like phases predicted previously at ambient pressure. The phonon spectra confirm that the six-membered rings

are stable. It is well known that temperature can be an important factor in determining the relative stability of structures[16]. We therefore tested the stability of the $Pna2_1$ phase at room temperature using *ab initio* molecular dynamics (AIMD) simulations with Parrinello-Rahman ($NpT$) dynamics and a Langevin thermostat[47,48]. As shown in Fig. 7, the drift in the statistical quantities during the 12 pico-second (ps) simulation are small. Due to the large cost of the AIMD calculations, we terminated the simulation after 12 ps, which was considered to be sufficient to confirm the stability of $Pna2_1$ at room temperature.

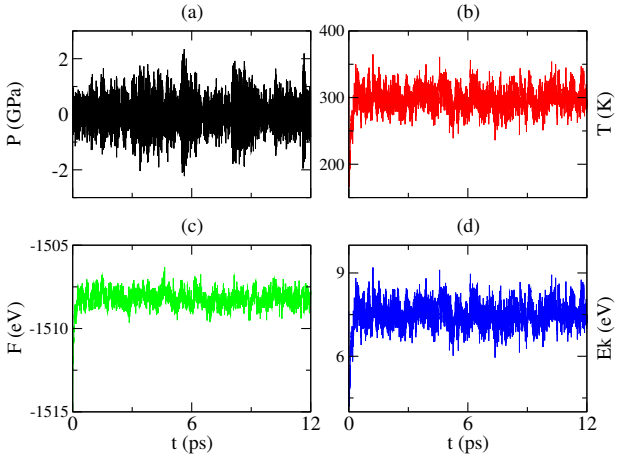


FIG. 7: Data from a molecular dynamics simulation at ambient pressure and 300 K for the $Pna2_1$ structure calculated using the $NpT$ ensemble. (a) the external pressure (P), (b) the temperature (T), (c) the free energy (F), (d) the kinetic energy ($E_k$).

## IV. CONCLUSION

Polymerization of molecular CO leads to the breaking of triple CO bonds under increasing pressure, and subsequently to structures with a mixture of double and single bonds, and at higher pressures to the dominance of single bonds. This leads to substantial changes in the energy and density of the material with pressure, and changes in the electronic structure. Although high pressure experimental polymerization of CO normally results in amorphous structures, careful control of the synthesis conditions or the use of other chemical methods may yield more ordered crystalline structures. The synthesis route remains a current challenge.

Extensive AIRSS calculations have led us to predict that several new CO structures are energetically more stable than previously-known structures over a wide range of pressures. Among them we find a chain-like polymeric phase consisting of six-membered rings (space group: $Pna2_1$) to be the most stable at low pressures. Using results from several different functionals we conclude that the $Pna2_1$ structure is more stable than molecular phases at ambient pressure. For example, results with the PBE-D3 (BJ) functional show that the $Pna2_1$ structure is about 0.814 eV/CO lower in enthalpy than the molecular $\alpha$ phase. The dynamical stability of the chain-like $Pna2_1$ phase is confirmed by phonon calculations at 0 GPa and by an *ab initio* molecular dynamics simulation at ambient pressure and temperature. The $Pna2_1$ structure is an insulator at zero pressure with a large band gap that we estimate to be about 3.6 eV. $Pna2_1$-CO is a potential "high energy density" material that can release about 4–9 times as much energy as TNT per mass.

### Acknowledgments

J.S. is grateful for financial support from the MOST of China (Grant Nos. 2016YFA0300404, 2015CB921202), the NSFC (Grant Nos. 51372112 and 11574133), the NSF of Jiangsu Province (Grant No. BK20150012), Special Program for Applied Research on Super Computation of the NSFC-Guangdong Joint Fund (the second phase), the Fundamental Research Funds for the Central Universities and Open Fund of Key Laboratory for Intelligent Nano Materials and Devices of the Ministry of Education (INMD-2016M01). C.J.P. and R.J.N. acknowledge financial support from the Engineering and Physical Sciences Research Council (EPSRC) of U.K. under grants [EP/G007489/2] (C.J.P.) and [EP/J017639/1] (R.J.N.). C.J.P. is also supported by the Royal Society through a Royal Society Wolfson Research Merit award. Some of the calculations were performed on the supercomputer in the High Performance Computing Center of Nanjing University and "Tianhe-2" at NSCC-Guangzhou.

* Electronic address: E-mail:jiansun@nju.edu.cn

[1] R. J. Hemley, Annu. Rev. Phys. Chem **51**, 763 (2000).
[2] V. Schettino and R. Bini, Phys. Chem. Chem. Phys. **5**, 1951 (2003).
[3] M. J. Lipp, W. J. Evans, B. J. Baer, and C. S. Yoo, Nature Mat. **4**, 211 (2005).
[4] C. S. Yoo, H. Cynn, F. Gygi, G. Galli, V. Iota, M. Nicol, S. Carlson, D. Hausermann, and C. Mailhiot, Phys. Rev. Lett. **83**, 5527 (1999).
[5] M. I. Eremets, A. G. Gavriliuk, N. R. Serebryanaya, I. A. Trojan, D. A. Dzivenko, R. Boehler, H. K. Mao, and R. J. Hemley, J. Chem. Phys. **121**, 11296 (2004).
[6] D. T. Cromer, D. Schiferl, R. Lesar, and R. L. Mills, Acta Cryst. Section C **39**, 1146 (1983).

[7] R. L. Mills, D. Schiferl, A. I. Katz, and B. W. Olinger, Journal de Physique **45**, 187 (1984).
[8] A. I. Katz, D. Schiferl, and R. L. Mills, J. Phys. Chem. **88**, 3176 (1984).
[9] R. L. Mills, B. Olinger, and D. T. Cromer, J. Chem. Phys. **84**, 2837 (1986).
[10] P. F. Fracassi, G. Cardini, S. Oshea, R. W. Impey, and M. L. Klein, Phys. Rev. B **33**, 3441 (1986).
[11] G. Frapper, C.-X. Cu, M. Kertesz, J.-F. Halet, J.-Y. Saillard, and M. Kertesz, Chem. Commun. pp. 2011–2012 (1997).
[12] M. Lipp, W. J. Evans, V. Garcia-Baonza, and H. E. Lorenzana, J. Low Temp. Phys. **111**, 247 (1998).
[13] S. Bernard, G. L. Chiarotti, S. Scandolo, and E. Tosatti, Phys. Rev. Lett. **81**, 2092 (1998).
[14] W. J. Evans, M. J. Lipp, C. S. Yoo, H. Cynn, J. L. Herberg, R. S. Maxwell, and M. F. Nicol, Chem. Mat. **18**, 2520 (2006).
[15] M. Ceppatelli, R. Bini, and V. Schettino, J. Phys. Chem. B **113**, 14640 (2009).
[16] J. Sun, D. D. Klug, C. J. Pickard, and R. J. Needs, Phys. Rev. Lett. **106**, 145502 (2011).
[17] C. Mailhiot, L. H. Yang, and A. K. Mcmahan, Phys. Rev. B **46**, 14419 (1992).
[18] J. Sun, M. Martinez-Canales, D. D. Klug, C. J. Pickard, and R. J. Needs, Phys. Rev. Lett. **111**, 175502 (2013).
[19] J. Sun, M. Martinez-Canales, D. D. Klug, C. J. Pickard, and R. J. Needs, Phys. Rev. Lett. **108**, 045503 (2012).
[20] V. Iota, C. S. Yoo, and H. Cynn, Science **283**, 1510 (1999).
[21] V. Iota, C. S. Yoo, J. H. Klepeis, Z. Jenei, W. Evans, and H. Cynn, Nature Mat. **6**, 34 (2007).
[22] M. B. Rubin and R. Gleiter, Chem. Rev. **100**, 1121 (2000).
[23] R. Peierls, *Surprises in theoretical physics* (Princeton, N.J.: Princeton University Press, 1979).
[24] X.-D. Wen, L. Hand, V. Labet, T. Yang, R. Hoffmann, N. W. Ashcroft, A. R. Oganov, and A. O. Lyakhov, Proc. Natl. Acad. Sci. U.S.A. **108**, 6833 (2011).
[25] K. AlKaabi, D. L. V. K. Prasad, P. Kroll, N. W. Ashcroft, and R. Hoffmann, J. Am. Chem. Soc. **136**, 3410 (2014).
[26] A. Hirata, S. Kohara, T. Asada, M. Arao, C. Yogi, H. Imai, Y. Tan, T. Fujita, and M. Chen, Nat. Commun. **7**, 11591 (2016).
[27] L. Allamandola, M. Bernstein, S. Sandford, and R. Walker, Space Sci. Rev. **90**, 219 (1999), ISSN 0038-6308, iSSI Workshop on Composition and Origin of Cometary Material, BERN, SWITZERLAND, SEP 14-18, 1998.
[28] M. Collings, J. Dever, H. Fraser, M. McCoustra, and D. Williams, Astrophys. J. **583**, 1058 (2003), ISSN 0004-637X.
[29] Y. Shi, J. Wang, Z.-Y. Zhang, Y. Gao, C.-N. Hao, X.-Y. Xia, and Q. Gu, Nat. Commun. **7**, 13789 (2016), ISSN 2041-1723.
[30] R. J. Needs and C. J. Pickard, APL Materials **4**, 053210 (2016).
[31] A. Dewaele, N. Worth, C. J. Pickard, R. J. Needs, S. Pascarelli, O. Mathon, M. Mezouar, and T. Irifune, Nature Chemistry **8**, 784 (2016).
[32] Y. Li, L. Wang, H. Liu, Y. Zhang, J. Hao, C. J. Pickard, J. R. Nelson, R. J. Needs, W. Li, Y. Huang, et al., Phys. Rev. B **93** (2016), ISSN 2469-9950.
[33] J. R. Nelson, R. J. Needs, and C. J. Pickard, Phys. Chem. Chem. Phys. **17**, 6889 (2015).
[34] C. J. Pickard and R. J. Needs, Phys. Rev. B **91**, 104101 (2015).
[35] Y. Zhou, J. Wu, W. Ning, N. Li, Y. Du, X. Chen, R. Zhang, Z. Chi, X. Wang, X. Zhu, et al., Proc. Natl. Acad. Sci. U.S.A. **113**, 2904 (2016).
[36] Y. Zhou, P. Lu, Y. Du, X. Zhu, G. Zhang, R. Zhang, D. Shao, X. Chen, X. Wang, M. Tian, et al., Phys. Rev. Lett. **117**, 146402 (2016), URL `http://link.aps.org/doi/10.1103/PhysRevLett.117.146402`.
[37] P. Lu, J.-S. Kim, J. Yang, H. Gao, J. Wu, D. Shao, B. Li, D. Zhou, J. Sun, D. Akinwande, et al., Phys. Rev. B **94**, 224512 (2016), URL `http://link.aps.org/doi/10.1103/PhysRevB.94.224512`.
[38] G. L. Weerasinghe, C. J. Pickard, and R. J. Needs, J. Phys.: Conden. Matter **27**, 45 (2015).
[39] Q. Hu, D. Y. Kim, Y. Wenge, L. Yang, L. Zhang, and H.-K. Mao, Nature **534**, 241 (2016).
[40] P. E. Blochl, Phys. Rev. B **50**, 17953 (1994).
[41] G. Kresse and D. Joubert, Phys. Rev. B **59**, 1758 (1999).
[42] G. Kresse and J. Furthmüller, Comp. Mat. Sci. **6**, 15 (1996).
[43] J. P. Perdew, K. Burke, and M. Ernzerhof, Phys. Rev. Lett. **77**, 3865 (1996).
[44] X. Gonze and C. Lee, Phys. Rev. B **55**, 10355 (1997).
[45] P. Giannozzi, S. Baroni, N. Bonini, M. Calandra, R. Car, C. Cavazzoni, D. Ceresoli, G. L. Chiarotti, M. Cococcioni, I. Dabo, et al., J. Phys.: Conden. Matter **21**, 395502 (2009).
[46] S. Grimme, J. Comput. Chem. **27**, 1787 (2006).
[47] M. Parrinello and A. Rahman, Phys. Rev. Lett. **45**, 1196 (1980).
[48] M. Parrinello and A. Rahman, J. Appl. Phys. **52**, 7182 (1981).
[49] C. J. Pickard and R. J. Needs, Phys. Rev. Lett. **97**, 045504 (2006).
[50] C. J. Pickard and R. J. Needs, J. Phys.: Conden. Matter **23**, 053201 (2011).
[51] J. Heyd and G. E. Scuseria, J. Chem. Phys. **121**, 1187 (2004).
[52] J. Heyd, G. E. Scuseria, and M. Ernzerhof, J. Chem. Phys. **124**, 219906 (2006).
[53] J. Paier, R. Hirschl, M. Marsman, and G. Kresse, J. Chem. Phys. **122**, 234102 (2005).
[54] J. Paier, M. Marsman, K. Hummer, G. Kresse, I. C. Gerber, and J. G. Angyan, J. Chem. Phys. **124**, 154709 (2006).
[55] S. Grimme, J. Antony, S. Ehrlich, and H. Krieg, J. Chem. Phys. **132**, 154104 (2010).
[56] S. Grimme, S. Ehrlich, and L. Goerigk, J. Comput. Chem. **32**, 1456 (2011).
[57] S. J. Clark, M. D. Segall, C. J. Pickard, P. J. Hasnip, M. J. Probert, K. Refson, and M. C. Payne, Z. Kristallogr. **220**, 567 (2005).
[58] G. Roman-Perez and J. M. Soler, Phys. Rev. Lett. **103**, 096102 (2009).
[59] J. Klimes, D. R. Bowler, and A. Michaelides, J. Phys.: conden. Matter **22**, 022201 (2010).
[60] J. Klimes, D. R. Bowler, and A. Michaelides, Phys. Rev. B **83**, 195131 (2011).
[61] T. Thonhauser, V. R. Cooper, S. Li, A. Puzder, P. Hyldgaard, and D. C. Langreth, Phys. Rev. B **76**, 125112 (2007).
[62] M. Dion, H. Rydberg, E. Schroder, D. C. Langreth, and B. I. Lundqvist, Phys. Rev. Lett. **92**, 246401 (2004).
[63] L. Vegard, Zeitschrift Fur Physik **61**, 185 (1930).
[64] A. Simon and K. Peters, Acta Crystallographica Section B-structural Science **36**, 2750 (1980).

[65] D. E. Nixon, G. S. Parry, and A. R. Ubbelohde, Proceedings of the Royal Society of London Series A-mathematical and Physical Sciences **291**, 324 (1966).
[66] K. D. Bronsema, J. L. Deboer, and F. Jellinek, Zeitschrift Fur Anorganische Und Allgemeine Chemie **541**, 15 (1986).
[67] K. Lee, E. D. Murray, L. Kong, B. I. Lundqvist, and D. C. Langreth, Phys. Rev. B **82**, 081101 (2010).